

Quantum dynamics in single spin measurement

Stefano Mancini* and David Vitali†

Dipartimento di Fisica, Università di Camerino, I-62032 Camerino, Italy.

Héctor Moya-Cessa‡

*INAOE, Coordinacion de Optica, Apdo. Postal 51 y 216,
72000 Puebla, Pue., Mexico,
and ICTP, Trieste, Italy*

(Dated: November 12, 2018)

We study the quantum dynamics of a model for the single-spin measurement in magnetic-resonance force microscopy. We consider an oscillating driven cantilever coupled with the magnetic moment of the sample. Then, the cantilever is damped through an external bath and its readout is provided by a radiation field. Conditions for reliable measurements will be discussed.

PACS numbers: 03.67.-a, 03.65.Ta, 76.60.-k

I. INTRODUCTION

Quantum state manipulation has become a fascinating perspective of modern physics. With concepts developed in atomic and molecular physics the field has been further stimulated by the possibility of quantum computation. For this purpose a number of individual two-state quantum systems (qubits) should be manipulated in a controlled way. Several physical realizations of qubits have been considered in recent years, but nano-electronic devices appear particularly promising because they can be embedded in circuit and scaled up to large number of qubits. In addition to manipulation, single qubit measurement is an important and delicate question. For instance, a force resolution of attonewtons is required to detect qubits represented by single spins [1]. Nowadays, magnetic resonance force microscopy (MRFM) is striving for this ultimate goal [2]. The use of cantilevers to detect small forces is at the heart of force microscopy in all its various forms [3]. Therefore, it is one of the most promising techniques to also achieve single spin detection.

Usually, small magnetic samples of unpaired electron spins are detected using a MRFM technique based on cyclic adiabatic inversion (CAI) [1, 4], and the quantum dynamics of measurement for this method has been recently discussed in [5, 6]. However, a new technique called “oscillating-cantilever-driven adiabatic reversals” (OSCAR) has been proposed and implemented in [7], where a sensitivity of about one hundred spins has been demonstrated. Very recently, this detection protocol has been improved and a sensitivity equivalent to a single electron spin has been finally achieved [8]. In the OSCAR protocol, the driven cantilever causes the adiabatic inversion of the paramagnetic moment of the sample. The backaction of this moment causes a frequency shift of the

cantilever, which is then detected by a fiber-optic interferometer. A classical description of the spin-cantilever dynamics in the OSCAR technique has been given in Ref. [9]. The quantum dynamics of the spin-cantilever system has been instead studied in Ref. [10], where the master equation including the decohering effect of a high-temperature environment has been solved numerically. The present paper investigates the quantum dynamics of the whole system including not only the spin and the cantilever, but also the effective measurement device, i.e., the fiber-optic interferometer, which is here represented by a quantized radiation mode. The spin state manifests itself in the probability distribution of the phase of the field and our treatment allows us to take into account also the backaction of the measurement meter (the field mode) on the spin-cantilever system. Differently from [10], our approach is based on the exact analytical solution of the quantum dynamics which is valid in the adiabatic limit and for not too large spin-cantilever coupling. The paper is organized as follows. In Section II we introduce the model, then in Section III we solve the quantum dynamics. In Section IV we present the main results. Section IV is for concluding remarks.

II. THE MODEL

We consider a model where a ferromagnetic particle is mounted on the cantilever tip. A permanent magnetic field B_z points in the z direction, while a rf field of magnitude B_1 rotates in the $x-y$ plane in resonance with the spin precession around z axis at frequency ω_s . A radiation field is then used to monitor the cantilever’s position. We describe the cantilever interacting with a single electron spin-1/2 as a harmonic oscillator of frequency ω_c , and the radiation field as a single electromagnetic mode of frequency ω_r . Then, the dimensionless Hamiltonian for such a system (scaled by the factor $\hbar\omega_c$) can be writ-

*Electronic address: stefano.mancini@unicam.it

†Electronic address: david.vitali@unicam.it

‡Electronic address: hmmc@inaoe.mx

ten as

$$\begin{aligned}
H &= a^\dagger a + \omega'_r b^\dagger b + \omega'_s S_z \\
&+ \epsilon [S_x \cos(\omega_s t) + S_y \sin(\omega_s t)] \\
&- \sqrt{2}\eta(a + a^\dagger)S_z - \kappa b^\dagger b(a + a^\dagger). \quad (1)
\end{aligned}$$

Here a is the ladder operator of the cantilever

$$a = \sqrt{\frac{k_c}{2\hbar\omega_c}} \left(Z + i\frac{\omega_c}{k_c} P \right), \quad (2)$$

where P and Z are the momentum and z -coordinate operators of the cantilever, and k_c is the cantilever spring constant. Moreover, b, b^\dagger are the ladder operators of the radiation mode with $[b, b^\dagger] = 1$, $\omega'_r = \omega_r/\omega_c$, $\omega'_s = \omega_s/\omega_c$, and S_i ($i = x, y, z$) are the usual spin operators obeying the commutation rule $[S_x, S_y] = 2iS_z$ and its cyclic permutations. The first row of Eq. (1) is the free Hamiltonian of the system, the second row is the driving term of amplitude ϵ given by [9, 10]

$$\epsilon = \frac{\gamma_e B_1}{\omega_c}, \quad (3)$$

where γ_e is the electron gyromagnetic ratio. Finally, the third row contains the spin-cantilever interaction (due to the spatially varying magnetic field B_z) with coupling constant [9, 10]

$$\eta = \frac{\gamma_e}{2} \sqrt{\frac{\hbar}{\omega_c k_c}} \left| \frac{\partial B_z}{\partial z} \right|, \quad (4)$$

and the optomechanical interaction (due to the radiation pressure force) with coupling constant κ , which, for a cavity interferometer with length L is given by [11]

$$\kappa = \frac{\omega_r}{L} \sqrt{\frac{\hbar}{2k_c\omega_c}}. \quad (5)$$

The Hamiltonian (1) in interaction picture with respect to $H_0 = \omega'_r b^\dagger b + \omega'_s S_z$ reads

$$H = a^\dagger a + \epsilon S_x - \sqrt{2}\eta(a + a^\dagger)S_z - \kappa b^\dagger b(a + a^\dagger), \quad (6)$$

which is the same model Hamiltonian considered in [10], supplemented with the optomechanical interaction with the readout radiation mode b . It is then convenient to apply the $\pi/2$ rotation around the y axis in the spin space $R = \exp[iS_y(\pi/4)]$ exchanging S_x and S_z , to obtain the transformed Hamiltonian

$$\begin{aligned}
\tilde{H} &\equiv RHR^\dagger \\
&= a^\dagger a + \epsilon S_z - \left(\sqrt{2}\eta S_x + \kappa b^\dagger b \right) (a + a^\dagger). \quad (7)
\end{aligned}$$

Apart from the additional optomechanical interaction term, Eq. (7) is equivalent to the Hamiltonian of a two-level atom with energy separation 2ϵ interacting with a quantized radiation mode with unit oscillation frequency,

represented by the cantilever z -motion [12]. The equivalent dipole-interaction term in Eq. (7) contains also counter-rotating terms, which are usually neglected in quantum optical situations (rotating wave approximation (RWA)) [12]. This approximation is however not justified in the present case. In fact, in typical MRFM situations, the spin is much faster than the cantilever and adiabatically follows the cantilever motion, i.e., $\epsilon \gg 1$. To be more precise, the OSCAR technique is usually operated under the adiabatic condition $\epsilon^2 \gg \eta\alpha_m$, where α_m is the mean amplitude of the cantilever oscillations, and under the full reversal condition $\epsilon \ll \eta\alpha_m$ [7, 10]. However, Ref. [10] shows that the best signal sensitivity is achieved for partial adiabatic reversals, i.e. $\epsilon \simeq \eta\alpha_m$. Along this line, we consider the limit $\epsilon \gg 1 + \eta$ together with $\kappa \ll 1$, which allow us to treat the interaction part of Eq. (7) as a small perturbation with respect to the free Hamiltonian $a^\dagger a + \epsilon S_z$. Thus, keeping the lowest nonzero order terms (first order in κ and second order in η), we end up with the effective Hamiltonian

$$\tilde{H}_{eff} = a^\dagger a + \epsilon S_z + \chi a^\dagger a S_z - \kappa b^\dagger b(a + a^\dagger), \quad (8)$$

where the effective spin-cantilever interaction χ is given by

$$\chi = \frac{16\eta^2\epsilon}{4\epsilon^2 - 1}. \quad (9)$$

The third term of Eq.(8), describes a dispersive interaction in which the spin and the cantilever energies are independently conserved and one induces a state-dependent phase shift on the other. In particular, the cantilever undergoes a frequency shift $\pm\chi$ depending upon the value of S_z , which is just the frequency shift which is detected in the OSCAR technique by means of a phase sensitive measurement of the radiation mode. Therefore we expect that by measuring the probability distribution of the field phase one effectively measures the spin component S_z , which corresponds to S_x in the initial, non-rotated frame. This is consistent with the classical description of MRFM [9], in which the cantilever always measures the spin component along the effective magnetic field which, in the strong adiabatic limit of very large ϵ considered here, is essentially aligned along the x direction.

III. QUANTUM DYNAMICS

To describe a realistic situation we consider the cantilever plunged in a thermal bath at equilibrium temperature T and subject to a viscous force with damping rate Γ (with $\Gamma/\omega_c \equiv \gamma$). This situation corresponds to an ohmic environment [13], and since for typical MRFM cantilevers ω_c is of order of some kHz, it is $N \equiv k_B T/\hbar\omega_c - 1/2 \gg 1$ (k_B is the Boltzmann's constant) even at cryogenic temperatures, so that environmental effects are satisfactorily

described in terms of the Caldeira-Leggett master equation [14], which is valid in the high temperature limit and is described by the superoperator [15]

$$\begin{aligned} \mathcal{L}\tilde{\rho} = & -\frac{\gamma}{4} [a + a^\dagger, \{a - a^\dagger, \tilde{\rho}\}] \\ & -\frac{\gamma k_B T}{2 \hbar \omega_c} [a + a^\dagger, [a + a^\dagger, \tilde{\rho}]] , \end{aligned} \quad (10)$$

where $\tilde{\rho}$ is the density matrix of the rotated system. Therefore, the complete system dynamics will be governed by the following master equation

$$\frac{d}{dt}\tilde{\rho} = -i [\tilde{H}_{eff}, \tilde{\rho}] + \mathcal{L}\tilde{\rho}, \quad (11)$$

where, due to the adoption of the dimensionless Hamiltonian of Eq. (8), time t is also dimensionless, i.e., scaled by ω_c .

In order to solve the master equation (11) we introduce the eigenstates $|e\rangle, |g\rangle$ of S_z with eigenvalues $+1, -1$ respectively, and we split the total density operator as

$$\begin{aligned} \tilde{\rho} = & \tilde{\rho}^{(ee)} \otimes |e\rangle\langle e| + \tilde{\rho}^{(gg)} \otimes |g\rangle\langle g| \\ & + \tilde{\rho}^{(eg)} \otimes |e\rangle\langle g| + \tilde{\rho}^{(ge)} \otimes |g\rangle\langle e| , \end{aligned} \quad (12)$$

with $\tilde{\rho}^{(ge)} = [\tilde{\rho}^{(eg)}]^\dagger$.

The terms $\tilde{\rho}^{(ij)}$ ($i, j = e, g$) in Eq. (12) can be expanded on the set of Fock states external product operators $|n\rangle_r \langle m|$ ($n, m \in \mathbf{N}$) for the radiation mode and on the continuous set of displacement operators $D_c(\lambda) = \exp\{\lambda a^\dagger - \lambda^* a\}$ ($\lambda \in \mathbf{C}$) for the cantilever mode, as follow [16]

$$\tilde{\rho}^{(ij)}(t) = \sum_{n,m=0}^{\infty} \int \frac{d^2\lambda}{\pi} e^{-|\lambda|^2/2} \Theta_{nm}^{(ij)}(\lambda, t) D_c^\dagger(\lambda) \otimes |n\rangle_r \langle m| , \quad (13)$$

where $\Theta_{nm}^{(ij)}(t)$ represent normally ordered characteristic functions [15, 16] for the cantilever mode for given spin and radiation states (they are explicitly given in the Appendix A).

From Eq. (12) one gets the non-rotated solution in the original frame

$$\begin{aligned} \rho(t) = & R^\dagger \tilde{\rho}(t) R \quad (14) \\ = & \frac{1}{2} [\tilde{\rho}^{(ee)}(t) + \tilde{\rho}^{(gg)}(t) - \tilde{\rho}^{(eg)}(t) - \tilde{\rho}^{(ge)}(t)] \otimes |e\rangle\langle e| \\ & + \frac{1}{2} [\tilde{\rho}^{(ee)}(t) + \tilde{\rho}^{(gg)}(t) + \tilde{\rho}^{(eg)}(t) + \tilde{\rho}^{(ge)}(t)] \otimes |g\rangle\langle g| \\ & + \frac{1}{2} [\tilde{\rho}^{(ee)}(t) - \tilde{\rho}^{(gg)}(t) + \tilde{\rho}^{(eg)}(t) - \tilde{\rho}^{(ge)}(t)] \otimes |e\rangle\langle g| \\ & + \frac{1}{2} [\tilde{\rho}^{(ee)}(t) - \tilde{\rho}^{(gg)}(t) - \tilde{\rho}^{(eg)}(t) + \tilde{\rho}^{(ge)}(t)] \otimes |g\rangle\langle e| . \end{aligned}$$

As initial condition we consider a coherent state $|\beta\rangle_r$ for the radiation field, while for the cantilever we consider a thermal state at temperature T , shifted by a complex amplitude α , where $\text{Re}\{\alpha\}$ gives the initial mean value of the position and $\text{Im}\{\alpha\}$ the initial mean value of the momentum.

IV. QUANTUM MEASUREMENT

As discussed above, the cantilever's position carries information about the spin state and, in turn, it is read by the radiation field. Due to the optomechanical coupling, the cantilever affects the phase of the field and we have therefore to look at the probability distribution of the latter. The canonical probability operator measure (POM) for phase measurement is [17]

$$\Pi(\theta) = \frac{1}{2\pi} |\theta\rangle_r \langle \theta| , \quad \text{with} \quad |\theta\rangle_r = \sum_{n=0}^{\infty} e^{in\theta} |n\rangle_r . \quad (15)$$

Hence, the phase probability distribution results

$$P(\theta, \tau) \equiv \text{Tr} \{ \Pi(\theta) \rho(\tau) \} = P_{ee}(\theta, \tau) + P_{gg}(\theta, \tau) , \quad (16)$$

where we have introduced the new time $\tau \equiv \gamma t$ which, due to the scaling chosen above, is a dimensionless time now scaled by the cantilever damping rate Γ , and

$$P_{jj}(\theta, \tau) = \text{Tr} \{ \Pi(\theta) \tilde{\rho}^{(jj)}(\tau) \} , \quad (17)$$

with $j = e, g$. From Eq. (13) we get

$$P_{jj}(\theta, \tau) = \frac{1}{2\pi} \sum_{n,m=0}^{\infty} e^{-i(n-m)\theta} \Theta_{nm}^{(jj)}(\lambda = 0, \tau) . \quad (18)$$

Let us now determine the conditions under which the apparatus performs reliable measurements of the spin. As discussed above, the apparatus is expected to measure S_x (in the original non-rotated frame) and therefore the easiest case is when the initial state of the spin is an eigenstate of S_x (in the non-rotated frame). We consider, for example, the eigenstate with $S_x = -1$, which correspond to state $|g\rangle$ in the rotated frame and therefore implying

$$\begin{aligned} \Theta_{nm}^{(jj)}(\lambda, \tau = 0) = & e^{-|\beta|^2} \frac{\beta^n (\beta^*)^m}{\sqrt{n!m!}} \\ & \times \exp \left\{ \alpha^* \lambda - \alpha^* \lambda - \frac{k_B T}{\hbar \omega_c} |\lambda|^2 \right\} \delta_{j,g} . \end{aligned} \quad (19)$$

As a consequence, $S_z = -1$ (in the rotated frame) is a constant of motion and one has a cantilever frequency shift χ (see Eq. (8)) which manifests itself as a shift of the phase distribution (see Fig. 1). In fact, the phase probability distribution is initially peaked around $\theta = 0$, due to the real amplitude ($\beta = 3$) of the initial coherent state of the radiation mode. Then the peak moves, toward larger values of θ , and faster than that with $\chi = 0$. If we had started from state $|e\rangle$ ($S_z = 1$ in the rotated frame), one would have a smaller phase shift of the peak. This could be surprising as one would expect a greater phase shift for frequency $(1 + \chi)$ and a smaller one for $(1 - \chi)$. However, if one just considers the unitary evolution arising from Eq.(8), one reduces to the model studied in Refs.[11],

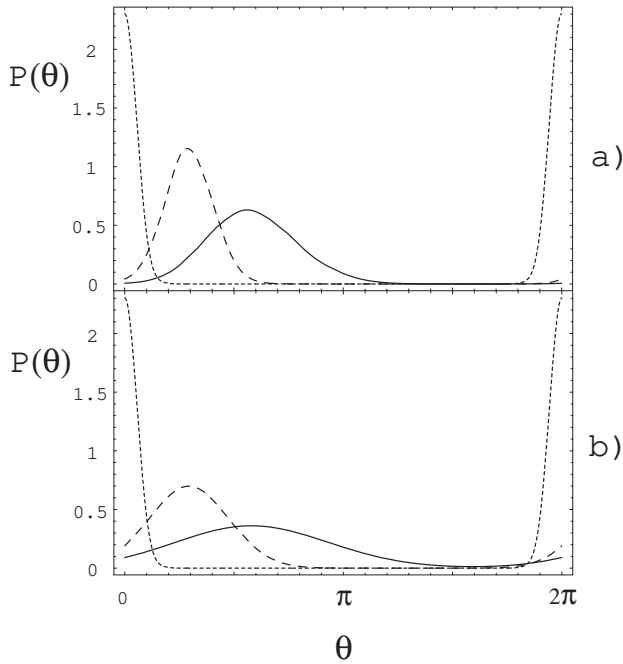


FIG. 1: Phase distribution for an initial state of the spin $(|g\rangle - |e\rangle)/\sqrt{2}$ (in the non-rotated frame) at times $\tau = 0$ (dotted line), $\tau = 8 \times 10^4$ (dashed and solid line). The dashed line refers to $\chi = 0$ while the solid line to $\chi = 0.5$. The values of other parameters are $\gamma = 10^{-4}$, $\kappa/\gamma = 0.08$, $\alpha = 4i$, $\beta = 3$, and $N = 10^2$ a), $N = 10^4$ b).

where it is possible to argue that the induced phase shift is inversely proportional to the cantilever's frequency.

In Fig. 1 we have considered two different values of temperature, $N = 10^2$ (a) and $N = 10^4$ (b), which for typical cantilever frequencies $\omega_c/2\pi \simeq 10^4$, correspond to $T \simeq 60 \mu\text{K}$ and $T \simeq 6 \text{ mK}$ respectively. One sees that already at mK temperatures the peak in the phase distribution corresponding to the state of the single spin starts to become too wide and flat to be clearly distinguished.

The conditions which the various parameters have to satisfy in order to have an unambiguous discrimination of the two spin eigenstates can be better established if we consider a different initial condition for the spin, i.e. an initial superposition of the two eigenstates of S_x (in the non-rotated frame). Fig. 2 refers to the initial condition $S_z = 1$ in the initial frame, corresponding to the state $(|g\rangle + |e\rangle)/\sqrt{2}$ in the rotated frame. This implies

$$\Theta_{nm}^{(jj)}(\lambda, \tau = 0) = e^{-|\beta|^2} \frac{\beta^n (\beta^*)^m}{\sqrt{n!m!}} \times \exp \left\{ \alpha^* \lambda - \alpha^* \lambda - \frac{k_B T}{\hbar \omega_c} |\lambda|^2 \right\}, \quad j = e, g \quad (20)$$

Due to the superposition, the measurement performed by the MRFM is reliable when we have the simultaneous presence of two distinct peaks in the phase distribution, associated with the two different phase shifts induced by

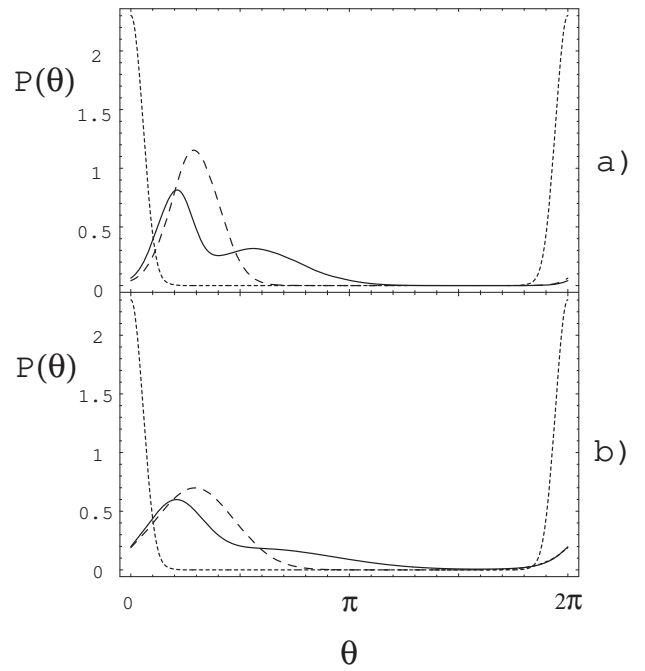


FIG. 2: Phase distribution for an initial state of the spin $|e\rangle$ (in the non-rotated frame) at times $\tau = 0$ (dotted line), $\tau = 8 \times 10^4$ (dashed and solid line). The dashed line refers to $\chi = 0$ while the solid line to $\chi = 0.5$. The values of other parameters are $\gamma = 10^{-4}$, $\kappa/\gamma = 0.08$, $\alpha = 4i$, $\beta = 3$, and $N = 10^2$ a), $N = 10^4$ b).

the two spin components. This means that the measurement time has not to be too small, in order to allow the two peaks to become distinguishable. This implies the condition $\chi t = \chi(\tau/\gamma) > 1$. Then, reliable measurement can be performed until the damping affects the dynamics, as it is confirmed by Fig. 2a, where one still has two distinct peaks corresponding to the two spin states when $\gamma\tau = 8$. In Fig. 2a the state of the single spin is well detected because we consider the low temperature condition $N = 10^2$, i.e., $T \simeq 60 \mu\text{K}$ (see above). At higher temperatures, the effect of the thermal environment is instead more destructive, as it can be seen from Fig. 2b, which corresponds to $N = 10^4$ ($T \simeq 6 \text{ mK}$), where the two peaks become too broad and are no more distinguishable.

The other parameter values in Figs. 1 and 2 are $\chi = 0.5$ and $\gamma = 10^{-4}$. This value of γ is realistic, because γ^{-1} corresponds to the cantilever's quality factor Q , which is even higher in recent experiments (see Ref. [8]), while the chosen value of χ is still far from present experimental values. In fact, from Eq. (9) one has $\chi \simeq 4\eta^2/\epsilon$ and using Eqs. (3) and (4) and the experimental values of Ref. [8], one gets $\epsilon \sim 800$, $\eta \sim 0.04$, so that $\chi \sim 10^{-5}$. Unfortunately, for such a small value of χ , the radiation field phase shift due to a single spin is too small to be detected and therefore larger values of χ , which means larger values of the coupling constant η , are needed to allow a

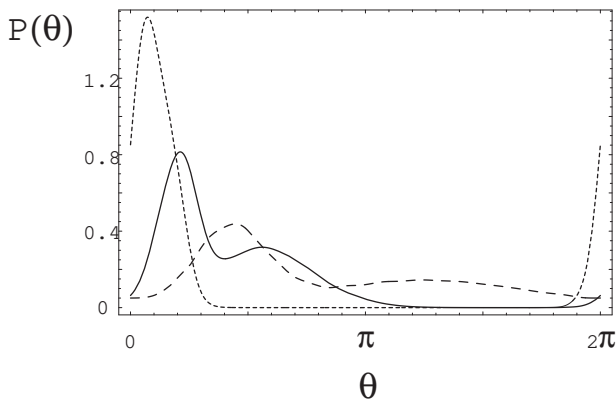


FIG. 3: Phase distribution for an initial state of the spin $|e\rangle$ (in the non-rotated frame) for different values of κ at time $\tau = 8 \times 10^4$. It is $\kappa/\gamma = 0.04$ dotted line, $\kappa/\gamma = 0.08$ solid line and $\kappa/\gamma = 0.12$ dashed line. The values of other parameters are $\gamma = 10^{-4}$, $\chi = 0.5$, $\alpha = 4i$, $\beta = 3$, $N = 10^2$.

reliable detection of the spin state within a reasonable detection time. Also a larger number of photons in the radiation mode would improve the resolution because in such a case the peaks in phase distributions would be narrower.

Finally, another important parameter is the optomechanical coupling κ between cantilever and the radiation readout mode. Similarly to χ , this parameter has to be sufficiently large, because otherwise the phase measurement has not enough sensitivity (see the dotted line in Fig. 3, where the two peaks are not well resolved). On the other hand, the readout mode is a quantum system and its backaction can blur the measurement result. This happens if the coupling κ is too large, as it is shown by the dashed line of Fig. 3. In this case the backaction is responsible for a phase diffusion of the peaks which are washed out and no more distinguishable. By inspection from Eq.(8) the condition $\kappa|\beta|^2 \ll |\alpha|^2$ should guarantee a negligible optomechanical backaction. However, it must be modified to take into account the elapsed time whenever the measurement is performed after many cycles, which naively implies $\kappa\tau|\beta|^2 \ll |\alpha|^2$ (confirmed by the values in Fig. 3).

V. CONCLUSIONS

We have presented a model for the description of the quantum dynamics of the measurement of a single spin by a MRFM operating with the OSCAR technique [7]. Our treatment includes also the phase-sensitive readout of the cantilever frequency-shift provided by a quantized radiation mode describing the measurement performed by an optical interferometer. We have solved analytically the dynamics in the strong adiabatic limit of a very fast spin, in which the spin reversal cannot be complete, in

the presence of a high-temperature ohmic environment acting on the cantilever. In this limit, the probability distribution of the phase of the optical readout mode gives a clear signature of the phase of the spin component along the effective magnetic field provided that the effective spin-cantilever coupling coefficient χ of Eq. (9) is sufficiently large and the optomechanical coupling κ is either not too large (in order to limit the backaction) or not too small (in order to extract information from the system).

Acknowledgments

H. M.-C. would like to thank the University of Camerino for the kind hospitality.

APPENDIX A

Since only $\Theta_{nm}^{(ee)}$ and $\Theta_{nm}^{(gg)}$ enter in Eq. (16), we need to solve Eq. (11) for $\tilde{\rho}^{(ee)}$ and $\tilde{\rho}^{(gg)}$ only.

1. Solution for $\tilde{\rho}^{(ee)}$

Let us define $\tilde{\rho}_{nm}^{(ee)} \equiv {}_r \langle n | \tilde{\rho}^{(ee)} | m \rangle_r$, then Eq. (11) can be rewritten in the form

$$\begin{aligned} \frac{d}{d\tau} \tilde{\rho}_{nm}^{(ee)} = & -i \frac{1+\chi}{\gamma} \left[a^\dagger a, \tilde{\rho}_{nm}^{(ee)} \right] \\ & + i \frac{\kappa}{\gamma} n (a + a^\dagger) \tilde{\rho}_{nm}^{(ee)} - i \frac{\kappa}{\gamma} m \tilde{\rho}_{nm}^{(ee)} (a + a^\dagger) \\ & - \frac{1}{4} \left[a^2 - (a^\dagger)^2, \tilde{\rho}_{nm}^{(ee)} \right] \\ & + \frac{1}{2} (N+1) \left(2a \tilde{\rho}_{nm}^{(ee)} a^\dagger - a^\dagger a \tilde{\rho}_{nm}^{(ee)} - \tilde{\rho}_{nm}^{(ee)} a^\dagger a \right) \\ & + \frac{1}{2} N \left(2a^\dagger \tilde{\rho}_{nm}^{(ee)} a - a a^\dagger \tilde{\rho}_{nm}^{(ee)} - \tilde{\rho}_{nm}^{(ee)} a a^\dagger \right) \\ & - \frac{1}{2} M \left(2a^\dagger \tilde{\rho}_{nm}^{(ee)} a^\dagger - (a^\dagger)^2 \tilde{\rho}_{nm}^{(ee)} - \tilde{\rho}_{nm}^{(ee)} (a^\dagger)^2 \right) \\ & - \frac{1}{2} M^* \left(2a \tilde{\rho}_{nm}^{(ee)} a - a^2 \tilde{\rho}_{nm}^{(ee)} - \tilde{\rho}_{nm}^{(ee)} a^2 \right), \quad (A1) \end{aligned}$$

with

$$N \equiv \frac{k_B T}{\hbar \omega_c} - \frac{1}{2}, \quad M \equiv -\frac{k_B T}{\hbar \omega_c}, \quad (A2)$$

and $\tau \equiv \gamma t$. Eq. (A1) is a valid master equation, preserving the positivity of the density matrix for $N(N+1) \geq |M|^2$ [15] which occurs in the high temperature limit, i.e. $k_B T \gg \hbar \omega_c$.

Since $\Theta_{nm}^{(ee)}$ represent normally ordered characteristic functions, we can transform Eq. (A1) into a partial dif-

ferential equation [15], that is

$$\begin{aligned} \frac{\partial}{\partial \tau} \Theta_{nm}^{(ee)} = & \left\{ \left(i \frac{1+\chi}{\gamma} - \frac{1}{2} \right) \lambda \frac{\partial}{\partial \lambda} \right. \\ & - \left(i \frac{1+\chi}{\gamma} + \frac{1}{2} \right) \lambda^* \frac{\partial}{\partial \lambda^*} \\ & + i \frac{\kappa}{\gamma} (n-m) \frac{\partial}{\partial \lambda} - i \frac{\kappa}{\gamma} (n-m) \frac{\partial}{\partial \lambda^*} \\ & - i \frac{\kappa}{\gamma} m \lambda - i \kappa n \lambda^* \\ & - \frac{1}{2} \lambda \frac{\partial}{\partial \lambda^*} - \frac{1}{2} \lambda^* \frac{\partial}{\partial \lambda} \\ & \left. - \frac{N}{2} \lambda^2 - \frac{N}{2} (\lambda^*)^2 - N |\lambda|^2 \right\} \Theta_{nm}^{(ee)}. \end{aligned} \quad (\text{A3})$$

We then use a Gaussian trial function, which is justified by the choice of an initial Gaussian state for the cantilever (a shifted thermal state) and by the fact that Eq. (A3) preserves Gaussian states,

$$\Theta_{nm}^{(ee)}(\tau) = \exp \left\{ A(\tau) \lambda + B(\tau) \lambda^* + C(\tau) |\lambda|^2 + D(\tau) \frac{\lambda^2}{2} + E(\tau) \frac{(\lambda^*)^2}{2} + F(\tau) \right\}. \quad (\text{A4})$$

As a consequence, Eq. (A3) yields the following set of linear differential equations

$$\begin{aligned} \dot{A}(\tau) = & \left(i\omega - \frac{1}{2} \right) A(\tau) - \frac{1}{2} B(\tau) \\ & - i \frac{\kappa}{\gamma} (n-m) (C(\tau) - D(\tau)) - i \frac{\kappa}{\gamma} m, \end{aligned} \quad (\text{A5})$$

$$\begin{aligned} \dot{B}(\tau) = & -\frac{1}{2} A(\tau) - \left(i\omega + \frac{1}{2} \right) B(\tau) \\ & + i \frac{\kappa}{\gamma} (n-m) (C(\tau) - E(\tau)) - i \frac{\kappa}{\gamma} n, \end{aligned} \quad (\text{A6})$$

$$\dot{C}(\tau) = -C(\tau) - \frac{1}{2} (E(\tau) + D(\tau)) - N, \quad (\text{A7})$$

$$\dot{D}(\tau) = -C(\tau) + (2i\omega - 1) D(\tau) - N, \quad (\text{A8})$$

$$\dot{E}(\tau) = -C(\tau) - (2i\omega + 1) E(\tau) - N, \quad (\text{A9})$$

$$\dot{F}(\tau) = i \frac{\kappa}{\gamma} (n-m) (A(\tau) - B(\tau)), \quad (\text{A10})$$

where we have set $\omega = (1+\chi)/\gamma$. Accordingly to Eq. (19), initial conditions now read

$$A(0) = \alpha^*, \quad (\text{A11})$$

$$B(0) = -\alpha, \quad (\text{A12})$$

$$C(0) = -\left(N + \frac{1}{2} \right), \quad (\text{A13})$$

$$D(0) = 0, \quad (\text{A14})$$

$$E(0) = 0, \quad (\text{A15})$$

$$F(0) = \ln \left[\frac{\beta^n (\beta^*)^m}{\sqrt{n!m!}} e^{-|\beta|^2} \right]. \quad (\text{A16})$$

Notice that

$$\Theta_{nm}^{(ee)}(\lambda = 0, \tau) = \text{Tr}_c \left\{ \tilde{\rho}^{(ee)} \right\} = e^{F(\tau)}. \quad (\text{A17})$$

Solving Eqs. (A5)-(A10) we get

$$\begin{aligned} F(\tau) = & F(0) + \frac{i(\kappa/\gamma)(n-m)}{4\omega^2 - 16\omega^4} \left\{ -2 \frac{F_1}{1+\Omega} \left[e^{-(1+\Omega)\tau/2} - 1 \right] - 2 \frac{F_2}{1-\Omega} \left[e^{-(1-\Omega)\tau/2} - 1 \right] \right. \\ & \left. - \frac{F_3}{1+\Omega} \left[e^{-(1+\Omega)\tau} - 1 \right] - \frac{F_4}{1-\Omega} \left[e^{-(1-\Omega)\tau} - 1 \right] + F_5 \left[e^{-\tau} - 1 \right] + F_6 \tau \right\}, \end{aligned} \quad (\text{A18})$$

where $\Omega^2 = 1 - 4\omega^2$ and

$$F_1 = \frac{\kappa}{\gamma}(n-m) \left[-4iN + 16iN\omega^2 \mp 8i\frac{\omega^2}{\Omega} (1+3N) \pm 32i\frac{\omega^4}{\Omega} (1+N) \pm 4i\frac{N}{\Omega} \right] \\ + \frac{\kappa}{\gamma}(n+m) \left[-2\omega + 8\omega^3 \pm 2\frac{\omega}{\Omega} \mp 8\frac{\omega^3}{\Omega} \right] \\ + \text{Re}\{\alpha\} \left[4\omega^2 \pm 16\omega^4 + 4\frac{\omega^2}{\Omega} \pm 16\frac{\omega^4}{\Omega} \right] + \text{Im}\{\alpha\} \left[8\frac{\omega^3}{\Omega} \pm 32\frac{\omega^5}{\Omega} \right], \quad (\text{A19})$$

$$F_3 = \frac{\kappa}{\gamma}(n-m) \left[-2i + 4i\omega^2 \pm 2i\frac{1}{\Omega} \mp 8i\frac{\omega^2}{\Omega} \right], \quad (\text{A20})$$

$$F_5 = 8i\omega^2\frac{\kappa}{\gamma}(n-m), \quad (\text{A21})$$

$$F_6 = \frac{\kappa}{\gamma}(n-m) [4i + 8iN - 16i\omega^2 - 32i\omega^2N] + \frac{\kappa}{\gamma}(n+m) [4\omega - 16\omega^3]. \quad (\text{A22})$$

2. Solution for $\tilde{\rho}^{(gg)}$

ω).

The quantities $\Theta_{nm}^{(gg)}(\lambda = 0, \tau)$ are given by Eqs.(A17)-(A22) with the replacement $\chi \rightarrow -\chi$ (hence $(1-\chi)/\gamma \rightarrow$

-
- [1] D. Rugar, O. Züger, S. Hoen, C. S. Yannoni, H. M. Vieth and R. D. Kendrick, *Science* **264**, 1560 (1994); J. A. Sidles, J. L. Garbini, K. L. Bruland, D. Rugar, O. Züger, S. Hoen and C. S. Yannoni *Rev. Mod. Phys.* **67**, 249 (1995).
 - [2] H. J. Mamin and D. Rugar, *Appl. Phys. Lett.* **79**, 3358 (2001).
 - [3] G. Binnig, C. F. Quate and C. Gerber, *Phys. Rev. Lett.* **56**, 930 (1986).
 - [4] K. Wago, D. Botkin, C.S. Yannoni, and D. Rugar, *Phys. Rev. B* **57**, 1108 (1998).
 - [5] G.P. Berman, F. Borgonovi, H.-S. Goan, S.A. Gurvitz, and V.I. Tsifrinovich, *Phys. Rev. B* **67**, 094425 (2003).
 - [6] T.A. Brun and H.-S. Goan, *Phys. Rev. A* **68**, 032301 (2003).
 - [7] B. C. Stipe, H. J. Mamin, C. S. Yannoni, T. D. Stowe, T. W. Kenny and D. Rugar, *Phys. Rev. Lett.* **87**, 277602 (2001).
 - [8] H. J. Mamin, R. Budakian, B. W. Chui, and D. Rugar, *Phys. Rev. Lett.* **91**, 207604 (2003); D. Rugar, R. Budakian, H. J. Mamin, and B. W. Chui, *Nature (London)* **430**, 329 (2004).
 - [9] G. P. Berman, D. I. Kamenev and V. I. Tsifrinovich, *Phys. Rev. A* **66**, 023405 (2002).
 - [10] G. P. Berman, F. Borgonovi, and V.I. Tsifrinovich, *Quantum Information and Computation* **4**, 102 (2004); arXiv:quant-ph/0306107.
 - [11] S. Mancini, V. I. Man'ko and P. Tombesi, *Phys. Rev. A* **55**, 3042 (1997); S. Bose, K. Jacobs and P. L. Knight, *Phys. Rev. A* **56**, 4175 (1997).
 - [12] C. Cohen-Tannoudji, J. Dupont-Roc, and G. Grynberg, *Atom-Photon Interactions: Basic Processes and Applications* (John Wiley & Sons, New York, 1992).
 - [13] A. O. Caldeira and A. J. Leggett, *Ann. Phys.* **149**, 374 (1983).
 - [14] A. O. Caldeira and A. J. Leggett, *Physica A* **121**, 187 (1987).
 - [15] C. W. Gardiner, *Quantum Noise*, (Springer, Berlin, 1991).
 - [16] K. E. Cahill and R. J. Glauber, *Phys. Rev.* **177**, 1882 (1969).
 - [17] D. F. Walls and G. J. Milburn, *Quantum Optics*, (Springer, Berlin, 1995).